Department of Mathematics and Statistics

Preprint MPCS-2019-07

11 October

Spectral estimates for saddle point matrices arising in weak constraint four-dimensional variational data assimilation

Ieva Daužickaitė*[1], Amos S. Lawless[1,2], Jennifer A. Scott[1,3], and Peter Jan van Leeuwen[1,2,4]

[1]School Of Mathematical, Physical and Computational Sciences, University of Reading,UK
[2] National Centre for Earth Observation, Reading, UK
[3]Scienti c Computing Department, STFC Rutherford Appleton Laboratory, UK
[4]Department of Atmospheric Science, Colorado State University, USA

Abstract

We consider the large-sparse symmetric linear systems of equations that arise in the solution of weak constraint four-dimensional variational data assimilation. These systems can be written as saddle point systems with a 3 3 block structure but block eliminations can be performed to reduce them to saddle point systems with a 2 2 block structure, or further to symmetric positive de nite systems. In this paper, we analyse how sensitive the spectra of these matrices are to the number of observations of the underlying dynamical system. We also obtain bounds on the eigenvalues of the matrices. Numerical experiments are used to con rm the theoretical analysis and bounds.

Keywords: data assimilation, saddle point systems, spectral estimates, weak constraint 4D-Var, sparse linear systems.

1 Introduction

Data assimilation estimates the state of a dynamical system by combining observations of the system with a prior estimate. The latter is called a background state and it is usually an output of a numerical model that simulates the dynamics of the system. The impact that the observations and the background state have on the state estimate depends on their errors whose statistical properties we assume are known. Data assimilation is used to produce initial conditions in numerical weather prediction (NWP) [22, 39], as well as other areas, e.g. ood forecasting [7], research into atmospheric composition [11], and neuroscience [27]. In operational applications, the process is made more challenging by the size of the system, e.g. the numerical model may be operating on 10^8 state variables and 10^5 10^6 observations may be incorporated [28, 23]. Moreover, there is usually a constraint on the time that can be spent on calculations.

The solution, called the analysis, is obtained by combining the observations and the background state in an optimal way. One approach is to solve a weighted least-squares problem, which requires minimising a cost function. An active research topic in this area is the weak constraint four-dimensional variational (4D-Var) data assimilation method [42, 43, 10, 5, 13, 16, 14]. It is employed in the search for states of the system over a time period, called the assimilation window. This method uses a cost function that is formulated under the assumption that the numerical model is not perfect and penalises the weighted discrepancy between the analysis and the observations, the analysis and the background state, and the di erence between the analysis and the trajectory given by integrating the dynamical model.

E ective minimisation techniques need evaluations of the cost function and its gradient that involve expensive operations with the dynamical model and its linearised variant. Such approaches are impractical in operational applications. One way to approximate the minimum of the weak constraint 4D-Var is to us86(are)vte4hauss-Newtonthemo the 1×1 block positive definite coefficient matrix depend on the available observations of the dynamical system. We present a novel examination of how adding new observations influence the spectrum of these coefficient matrices.

In Section 2, we formulate the data assimilation problem and introduce weak constraint 4D-Var with the 3×3 block and 2×2 block saddle point formulations and the 1×1 block symmetric positive definite formulation. Eigenvalue bounds for the saddle point and positive definite matrices and results on how the extreme eigenvalues and the bounds depend on the number of observations are presented in Section 3. Section 4 illustrates the theoretical considerations using numerical examples, and concluding remarks and future directions are presented in Section 5.

2 Variational Data Assimilation

The state of the dynamical system of interest at times $t_0 < t_1 < \dots < t_N$ is represented by the state vectors $x_0, x_1, \dots, x_N$ with $x_i \in \mathbb{R}^n$. A nonlinear model m_i that is assumed to have errors describes the transition from the state at time t_i to the state at time t_{i+1}, i.e.

$$x_{i+1} = m_i(x_i) + \epsilon_{i+1}, \qquad (1)$$

where ϵ_i represents the model error at time t_i. It is further assumed that the model errors are Gaussian with zero mean and covariance matrix $Q_i \in \mathbb{R}^{n \times n}$, and that they are uncorrelated in time, i.e. there is no relationship between the model errors at different times. In NWP, the model comes from the discretization of the partial differential equations that describe the flow and thermodynamics of a stratified multiphase fluid in interaction with radiation [22]. It also involves parameters that characterize processes arising at spatial scales that are smaller than the distance between the grid points [31]. Errors due to the discretization of the equations, errors in the boundary conditions, inaccurate parameters etc. are components of the model error [19].

The background information about the state at time t_0 is denoted by $x^b \in \mathbb{R}^n$. x^b usually comes from a previous short range forecast and is chosen to be the first guess of the state. It is assumed that the background term has errors that are Gaussian with zero mean and covariance matrix $B \in \mathbb{R}^{n \times n}$.

Observations of the dynamical system at time t_i are given by $y_i \in \mathbb{R}^{p_i}$. In NWP, there are considerably fewer observations than state variables, i.e. $p_i << n$. Also, there may be indirect observations of the variables in the state vector and a comparison is obtained by mapping the state variables to the observation space using a nonlinear operator $\mathcal{H}_i$. For example, satellite observations used in NWP provide top of the atmosphere radiance data, whereas the model operates on different meteorological variables, e.g. temperature, pressure, wind etc. [1] Hence, values of meteorological variables are transformed into top of the atmosphere radiances in order to compare the model output with the observations. In this case, the operator $\mathcal{H}_i$ is nonlinear and complicated. Approximations made when mapping the state variables to the observation space, different spatial and temporal scales between the model and some observations (observations may give information at a finer resolution than the model), and pre-processing, or quality control, of the observations (see, e.g. Section 5.8 of Kalnay [22]) comprise the representativity error [21]. The observation error is made up of the representativity error combined with the error arising due to the limited precision of the measurements. It is assumed to be Gaussian with zero mean and covariance matrix $R_i \in \mathbb{R}^{p_i \times p_i}$. The observation errors are assumed to be uncorrelated in time [23].

2.1 Weak constraint 4D-Var

In weak constraint 4D-Var, the analysis $x_0^a, x_1^a, \dots, x_N^a$ is obtained by minimising the following nonlinear cost function

$$J(x_0, x_1, \dots, x_N) = \frac{1}{2}(x_0 - x^b)^T B^{-1}(x_0 - x^b) + \frac{1}{2}\sum_{i}^{N} x_i(x_i$$ u7 Td4]TJ/F12 5.7999 T11(1)]T8 ET q 1 0 0 1 205.173 271.6

2.2 Incremental formulation

2.2.1 3×3 block saddle point formulation

In pursuance of exploiting parallel computations in data assimilation, Fisher and Gürol [13] proposed obtaining the state increment δx by solving a saddle point system (see also Freitag and Green [14]). New variables are introduced

$$\lambda = D^{-1}(b - L\,\delta x) \in \mathbb{R}^{(N+1)\,n}; \tag{6}$$

$$\mu = R^{-1}(d - H\,\delta x) \in \mathbb{R}^{p}. \tag{7}$$

The gradient of the cost function (5) with respect to δx provides the optimality constraint

$$\begin{aligned} 0 &= L^T D^{-1}(L\,\delta x - b) + H^T R^{-1}(H\,\delta x - d) \\ &= -(L^T \lambda + H^T \mu). \end{aligned} \tag{8}$$

Multiplying (6) by D and (7) by R together with (8), yields a coupled linear system of equations:

$$A_3 \begin{pmatrix} \lambda \\ \mu \\ \delta x \end{pmatrix} = \begin{pmatrix} b \\ d \\ 0 \end{pmatrix}, \tag{9}$$

where the coefficient matrix is given by

$$A_3 = \begin{pmatrix} D & 0 & L \\ 0 & R & H \\ L^T & H^T & 0 \end{pmatrix} \in \mathbb{R}^{(2(N+1)\,n+p) \times (2(N+1)\,n+p)}. \tag{10}$$

A_3 is a sparse symmetric indefinite saddle point matrix that has a 3×3 block form. Such systems are explored in the optimization literature [18, 25, 26]. When iteratively solving these systems, it is usually assumed that calculations involving the blocks on the diagonal are computationally expensive, while the off-diagonal blocks are cheap to apply and easily approximated. However, in our application, operations with the diagonal blocks are relatively cheap and the off-diagonal blocks are computationally expensive, particularly because of the integrations of the model and its adjoint in L and L^T.

Recall that the sizes of the blocks R, H and H^T depend on the number of observations p. Thus, the size of A_3 and possibly some of its characteristics are also affected by p. The saddle point systems that arise in different outer loops vary in the right hand sides and the linearisation states of L and H.

2.2.3 1×1 block formulation

The 2×2 block system can be further reduced to a 1×1 block system, that is, to the standard formulation (see, e.g., Trémolet [42] and A. El-Said [10] for a more detailed consideration):

$$(L^T D^{-1} L + H^T R^{-1} H)\, x = L^T D^{-1} b + H^T R^{-1} d.$$

Observe that the coefficient matrix

$$\begin{aligned} A_1 &= L^T D^{-1} L + H^T R^{-1} H \\ &= \begin{pmatrix} L^T & H^T \end{pmatrix} \begin{pmatrix} D^{-1} & 0 \\ 0 & R^{-1} \end{pmatrix} \begin{pmatrix} L \\ H \end{pmatrix} \end{aligned} \tag{13}$$

is the negative Schur complement of $\begin{pmatrix} D & 0 \\ 0 & R \end{pmatrix}$ in A_3. The matrix A_1 is block tridiagonal and symmetric positive definite, hence the conjugate gradient method by Hestenes and Stiefel [20] can be used. The computations with the linearised model in L at every time step can again be performed in parallel. However, the adjoint of the linearised model in L^T can only be applied after the computations with the model are finished, thus limiting the potential for parallelism.

3 Eigenvalues of the saddle point formulations

The rate of convergence of Krylov subspace iterative solvers for symmetric systems depends on the spectrum of the coefficient matrix (see, for example, Section 10 in the survey paper [3] and Lectures 35 and 38 in the textbook [41] for a discussion). Simoncini and Szyld [37] have shown that any eigenvalues of the saddle point systems that lie close to the origin can cause the iterative solver MINRES to stagnate for a number of iterations while the rate of convergence can improve if the eigenvalues are clustered.

In the following, we examine how the eigenvalues of the 3×3, 2×2 and 1×1 block matrices A_3, A_2, and A_1 change when new observations are added. This is done by considering the shift in the extreme eigenvalues of these matrices, that is the smallest and largest positive and negative eigenvalues. We then present bounds for the eigenvalues of these matrices. The bounds for the spectrum of A_3 are obtained by exploiting the earlier work of Rusten and Winther [32]. We derive bounds for the intervals that contain the spectra of A_2 and A_1.

3.1 Preliminaries

In order to determine how changing the number of observations influences the spectra of A_3, A_2, and A_1, we explore the extreme singular values and eigenvalues of some blocks in A_3, A_2 and A_1. We state two theorems that we will require. Here we employ the notation $\lambda_k(A)$ to denote the k-th largest eigenvalue of a matrix A and subscripts min and max are used to denote the smallest and largest eigenvalues, respectively.

Theorem 1 (See Section 8.1.2 of Golub and Van Loan [15]) If A and C are $n \times n$ Hermitian matrices, then

$$\lambda_k(A) + \lambda_{min}(C) \le \lambda_k(A + C) \le \lambda_k(A) + \lambda_{max}(C); \quad k \in \{1, 2, \ldots, n\}.$$

Theorem 2 (Cauchy's Interlace Theorem, see Theorem 4.2 in Chapter 4 of Stewart and Sun [38]) If A is an $n \times n$ Hermitian matrix and C is a $(n-1) \times (n-1)$ principal submatrix of A (a matrix obtained by eliminating a row and a corresponding column of A), then

$$\lambda_n(A) \le \lambda_{n-1}(C) \le \lambda_{n-1}(A) \le \cdots \le \lambda_2(A) \le \lambda_1(C) \le \lambda_1(A).$$

In the following lemmas we describe how the smallest and largest singular values of $(L^T \; H^T)$ (here L and H are as defined in Section 2.2) and the extreme eigenvalues of the observation error covariance matrix R change when new observations are introduced. The same is done for the largest eigenvalues of $H^T R^{-1} H$ assuming that R is diagonal. In these lemmas the subscript $k \in \{0, 1, \ldots, (N+1)n - 1\}$ denotes the number of available observations and the subscript $k+1$ indicates that a new observation is added to the system with k observations, i.e. matrices $R_k \in$

Proof. We consider the eigenvalues of $L^T L + H_k^T H_k$ and $L^T L + H_{k+1}^T H_{k+1}$, which are the squares of the singular values of $(L^T\ H_k^T)$ and $(L^T\ H_{k+1}^T)$, respectively (see Section 2.4.2 of Golub and Van Loan [15]). We can write

$$H_{k+1}^T H_{k+1} = \begin{pmatrix} H_k^T & h_{k+1} \end{pmatrix} \begin{pmatrix} H_k \\ h_{k+1}^T \end{pmatrix} = H_k^T H_k + h_{k+1} h_{k+1}^T .$$

Then by Theorem 1,

$$\sigma_{\min}^2 + \lambda_{\min}(h_{k+1} h_{k+1}^T) \le \sigma_{\min}^2 ; \quad k \in \{0, 1, \ldots, (N+1)n - 1\};$$

and since $h_{k+1} h_{k+1}^T$ is a rank 1 symmetric positive semidefinite matrix, $\lambda_{\min}(h_{k+1} h_{k+1}^T) = 0$.

The proof for the largest singular values is analogous. □

Lemma 2. Consider the observation error covariance matrices $R_k \in \mathbb{R}^{k \times k}$ and $R_{k+1} \in \mathbb{R}^{(k+1) \times (k+1)}$. Then

$$\lambda_{\min}(R_{k+1}) \le \lambda_{\min}(R_k) \quad \text{and} \quad \lambda_{\max}(R_k) \le \lambda_{\max}(R_{k+1}); \quad k \in \{0, 1, \ldots, (N+1)n - 1\};$$

i.e. the largest (respectively, smallest) eigenvalue of R increases (respectively, decreases), or is unchanged when new observations are introduced.

Proof. When adding an observation, a row and a corresponding column are appended to R_k while the other entries of R_k are unchanged. The result is immediate by applying Theorem 2. □

Lemma 3. If the observation errors are uncorrelated, i.e. R is diagonal, then

$$\lambda_{\max}(H_k^T R_k^{-1} H_k) \le \lambda_{\max}(H_{k+1}^T R_{k+1}^{-1} H_{k+1}); \quad k \in \{0, 1, \ldots, (N+1)n - 1\};$$

i.e. for diagonal R, the largest eigenvalue of $H^T R^{-1} H$ increases or is unchanged when new observations are introduced.

Proof. The proof is similar to that of Lemma 1. For diagonal R_{k+1}:

$$R_{k+1}^{-1} = \begin{pmatrix} R_k^{-1} & \\ & \sigma^{-1} \end{pmatrix}; \quad \sigma > 0.$$

Then

$$H_{k+1}^T R_{k+1}^{-1} H_{k+1} = \begin{pmatrix} H_k^T & h_{k+1} \end{pmatrix} \begin{pmatrix} R_k^{-1} & \\ & \sigma^{-1} \end{pmatrix} \begin{pmatrix} H_k \\ h_{k+1}^T \end{pmatrix} = H_k^T R_k^{-1} H_k + \sigma^{-1} h_{k+1} h_{k+1}^T .$$

Hence, by Theorem 1,

$$\lambda_{\max}(H_k^T R_k^{-1} H_k) + \sigma^{-1} \lambda_{\min}(h_{k+1} h_{k+1}^T) \le \lambda_{\max}(H_{k+1}^T R_{k+1}^{-1} H_{k+1}); \quad k \in \{0, 1, \ldots, (N+1)n - 1\};$$

3.2 Bounds for the 3×3 block formulation

To determine the numbers of positive and negative eigenvalues of A_3 given in (10), we write A_3 as a congruence transformation

$$
\begin{aligned}
A_3 = \begin{pmatrix} D & 0 & L \\ 0 & R & H \\ L^T & H^T & 0 \end{pmatrix} &= \begin{pmatrix} D & 0 & 0 \\ 0 & R & 0 \\ L^T & H^T & I \end{pmatrix} \begin{pmatrix} D^{-1} & 0 & 0 \\ 0 & R^{-1} & 0 \\ 0 & 0 & -L^T D^{-1} L - H^T R^{-1} H \end{pmatrix} \begin{pmatrix} D & 0 & L \\ 0 & R & H \\ 0 & 0 & I \end{pmatrix} \\
&= \hat{L} \hat{B} \hat{L}^T;
\end{aligned}
$$

where $I \in \mathbb{R}^{(N+1)n \times (N+1)n}$ is the identity matrix. Thus, by Sylvester's law of inertia (see Section 8.1.5 of Golub and Van Loan [15]), A_3 and $\hat{B}$ have the same inertia, i.e. the same number of positive, negative, and zero eigenvalues. Since the blocks D^{-1}, R^{-1} and $L^T D^{-1} L + H^T R^{-1} H = A_1$ are symmetric positive definite matrices, A_3 has $(N+1)n + p$ positive and $(N+1)n$ negative eigenvalues. In the following theorem, we explore how the extreme eigenvalues of A_3 change when new observations are introduced.

Theorem 3. *The smallest and largest negative eigenvalues of A_3 either move away from the origin or are unchanged when new observations are introduced. The same holds for the largest positive eigenvalue, while the smallest positive eigenvalue approaches the origin or is unchanged.*

Proof. Let $A_{3;k}$ denote A_3 where $p = k$. To account for an additional observation, a row and a corresponding column is added to A_3, hence $A_{3;k}$ is a principal submatrix of $A_{3;k+1}$. Let

$$\lambda_{-(N+1)n}(A_{3;k}) \le \lambda_{-((N+1)n-1)}(A_{3;k}) \le \dots \le \lambda_{-1}(A_{3;k}) < 0 < \lambda_1(A_{3;k}) \le \dots \le \lambda_{(N+1)n+k}(A_{3;k})$$

be the eigenvalues of $A_{3;k}$, and

$$\lambda_{-(N+1)n}(A_{3;k+1}) \le \lambda_{-((N+1)n-1)}(A_{3;k+1}) \le \dots \le \lambda_{-1}(A_{3;k+1}) < 0 < \lambda_1(A_{3;k+1}) \le \dots \le \lambda_{(N+1)n+k+1}(A_{3;k+1})$$

be the eigenvalues of $A_{3;k+1}$. Then by Theorem 2:

$$
\begin{aligned}
\text{smallest negative eigenvalues} \quad & \lambda_{-(N+1)n}(A_{3;k+1}) \le \lambda_{-(N+1)n}(A_{3;k}); \\
\text{largest negative eigenvalues} \quad & \lambda_{-1}(A_{3;k+1}) \le \lambda_{-1}(A_{3;k}); \\
\text{smallest positive eigenvalues} \quad & \lambda_{1}(A_{3;k+1}) \le \lambda_{1}(A_{3;k}); \\
\text{largest positive eigenvalues} \quad & \lambda_{(N+1)n+k}(A_{3;k}) \le \lambda_{(N+1)n+k+1}(A_{3;k+1}).
\end{aligned}
$$

□

To obtain information on not only how the eigenvalues of A_3 change because of new observations, but also on

Corollary 2. If $_{max} = {}_{max}$, the upper bound for the negative eigenvalues of A_3 in (16) is either unchanged or moves away from the origin when new observations are added. If $_{min} = {}_{min}$, the same holds for the lower bound for negative eigenvalues in (16).

Proof. The results follow from the facts that $_{max}$ and $_{min}$ do not change if observations are added, whereas $_{min}$ and $_{max}$ increase or are unchanged by Lemma 1. □

If $_{max} = {}_{max}$ or $_{min} = {}_{min}$, it is unclear how the interval for the negative eigenvalues in (16) changes, because $\sqrt{{}^2_{min} + 4\,{}^2_{max}}$ can increase, decrease or be unchanged, and both $_{max}$ and $\sqrt{{}^2_{max} + 4\,{}^2_{min}}$ can increase or be unchanged.

3.3 Bounds for the 2 2 block formulation

A_2 given in (12) is equal to the following congruence transformation

$$A_2 = \begin{pmatrix} D & L \\ L^T & H^T R^{\ 1} H \end{pmatrix} = \begin{pmatrix} D & 0 \\ L^T & I \end{pmatrix} \begin{pmatrix} D^{\ 1} & 0 \\ 0 & L^T D^{\ 1} L \quad H^T R^{\ 1} H \end{pmatrix} \begin{pmatrix} D & L \\ 0 & I \end{pmatrix};$$

where $I\ 2\ R^{(N+1)n\ \ (N+1)n}$ is the identity matrix. Then by Sylvester's law, A_2 has $(N+1)n$ positive and $(N+1)n$ negative eigenvalues. The change of the extreme negative and positive eigenvalues of A_2 due to the additional observations is analysed in the subsequent theorem. However, the result holds only in the case of uncorrelated observation errors, unlike the general analysis for A_3 in Theorem 3.

Theorem 5. If the observation errors are uncorrelated, i.e. R is diagonal, then the smallest and largest negative eigenvalues of A_2 either move away from the origin or are unchanged when new observations are added. Contrarily, the smallest and largest positive eigenvalues of A_2 approach the origin or are unchanged.

Proof. Matrices D and L do not depend on the number of observations. In Lemma 3, we have shown that $H^T_{k+1} R^{\ 1}_{k+1} H_{k+1} = H^T_k R_k^{\ 1} H_k + \ {}^{1} h_{k+1} h^T_{k+1};\ (\ > 0)$ for diagonal R. Hence, when $A_{2;k}$ denotes A_2 with $p = k$, we can write

$$A_{2;k+1} = A_{2;k} + \begin{pmatrix} 0 & 0 \\ 0 & {}^{1} h_{k+1} h^T_{k+1} \end{pmatrix} = A_{2;k} + E_2;$$

where E_2 has negative and zero eigenvalues. Let

$$_{(N+1)n}(A_{2;k}) \qquad _1(A_{2;k}) < 0 < \ _1(A_{2;k}) \qquad _{(N+1)n}(A_{2;k})$$

be the eigenvalues of $A_{2;k}$, and

$$_{(N+1)n}(A_{2;k+1}) \qquad _1(A_{2;k+1}) < 0 < \ _1(A_{2;k+1}) \qquad _{(N+1)n}(A_{2;k+1})$$

be the eigenvalues of $A_{2;k+1}$. By Theorem 1,

smallest negative eigenvalues $\ _{(N+1)n}(A_{2;k}) \quad {}^{1}\ _{max}(h_{k+1} h^T_{k+1}) \quad _{(N+1)n}(A_{2;k+1}) \quad _{(N+1)n}(A_{2;k});$

largest negative eigenvalues $\ _1(A_{2;k}) \quad {}^{1}\ _{max}(h_{k+1} h^T_{k+1}) \quad _1(A_{2;k+1}) \quad _1(A_{2;k});$

smallest positive eigenvalues $\ _1(A_{2;k}) \quad {}^{1}\ _{max}(h_{k+1} h^T_{k+1}) \quad _1(A_{2;k+1}) \quad _1(A_{2;k});$

largest positive eigenvalues $\ _{(N+1)n}(A_{2;k}) \quad {}^{1}\ _{max}(h_{k+1} h^T_{k+1}) \quad _{(N+1)n}(A_{2;k+1}) \quad _{(N+1)n}(A_{2;k}):$

□

We further search for the intervals in which the negative and positive eigenvalues of A_2 lie. We follow a similar line of thought as in Silvester and Wathen [35], with the energy arguments for any non-zero vector $w\ 2\ R^{(N+1)n}$

$$_{min}\ jjwjj^2 \quad w^T D w \quad _{max}\ jjwjj^2; \tag{18}$$

$$_{max}\ jjwjj^2 \quad w^T H^T R^{\ 1} H w \quad _{min}\ jjwjj^2; \tag{19}$$

$$_{min}\ jjwjj \quad jj\ L^T w jj \quad _{max}\ jjwjj; \tag{20}$$

$$_{min}\ jjwjj \quad jj\ (L^T \ H^T)^T w jj \quad _{max}\ jjwjj: \tag{21}$$

Theorem 6. The negative eigenvalues of A_2 lie in the interval

$$I = \frac{1}{2}\ \ _{min}\ \ _{max} \ \sqrt{(\ _{min} + \ _{max})^2 + 4\ {}^2_{max}}\ ;\min f\ _1; \max f\ _2;\ _3gg\ ; \tag{22}$$

where

$$ {}_1 = \frac{1}{2} \quad {}_{max} \quad {}_{min} \quad \sqrt{({}_{max} + {}_{min})^2 + 4 \, {}^{2}_{min}} \quad ; \tag{23}$$

$$ {}_2 = \quad {}^{1}_{max} \, {}^{2}_{min} \, ; \tag{24}$$

$$ {}_3 = \frac{1}{2} \quad {}_{max} \quad \sqrt{ {}^{2}_{max} + 4 \, {}^{2}_{min}} \quad ; \tag{25}$$

and the positive ones lie in the interval

$$ I_{+} = \frac{1}{2} \quad {}_{min} \quad {}_{max} + \sqrt{({}_{min} + {}_{max})^2 + 4 \, {}^{2}_{min}} \; ; \frac{1}{2} \quad {}_{max} \quad {}_{min} + \sqrt{({}_{max} + {}_{min})^2 + 4 \, {}^{2}_{max}} \quad : \tag{26}$$

Proof. Assume that $(u^T; v^T)^T; \; u; v \; 2 \; R^{(N+1) \, n}$ is an eigenvector of A_2 with an eigenvalue . Then the eigenvalue equations are

$$ Du + Lv = \; u; \tag{27}$$

$$ L^T u \quad H^T R \; {}^1 Hv = \; v: \tag{28}$$

We note that if $u = 0$ then $v = 0$ by (27) and if $v = 0$ then $u = 0$ by (28). Hence, $u; v \; 6 \; 0$.

First, we consider > 0. Equation (28) gives $v = (I \; + H^T R \; {}^1 H) \; {}^1 L^T u$, where $I \; 2 \; R^{(N+1) \, n \quad (N+1) \, n}$. The matrix $I \; + H^T R \; {}^1 H$ is positive de nite, hence nonsingular. We multiply (27) by u^T and use the previous expression for v to get

$$ u^T Du + u^T L (I \; + H^T R \; {}^1 H) \; {}^1 L^T u = \; jjujj $$

We obtain an alternative upper bound for the negative eigenvalues, that depends on the observational information and might be useful for the fully observed case, too. Equation (30) may be written as

$$||v||^2 = v^T (L^T \quad H^T) \begin{pmatrix} (D \quad I)^{1} & 0 \\ 0 & R^{1} \end{pmatrix} \begin{pmatrix} L \\ H \end{pmatrix} v:$$

Using (21) the previous equation gives inequality

$$^{2}_{min} \; ;$$

where $= \min f \; ^{1}_{max}; (\quad + \quad _{max})^{1} g$. If $= \; ^{1}_{max}$, the upper bound is

$$^{1}_{max} \; ^{2}_{min} = \; _2:$$

If $= (\quad + \quad _{max})^{1}$, the following inequality

$$^{2} \quad _{max} \quad ^{2}_{min} \quad 0$$

gives the bound

$$\frac{1}{2} \quad _{max} \quad \sqrt{^{2}_{max} + 4 \; ^{2}_{min}} \quad = \; _3:$$

Hence,

$$\max f \; _2; \; _3 g: \tag{32}$$

The required upper bound follows from (31) and (32)

Next, we obtain the lower bound for the negative eigenvalues. Using equation (30) with the largest eigenvalue of $(D \quad I)^{1}$ and other parts of (19) and (20) yields

$$||v||^2 \quad ^{2}_{max} ||v||^2 \frac{1}{_{min}} + \; _{max} ||v||^2:$$

Solving

$$^{2} \quad (\; _{min} \quad _{max}) \quad _{max} \quad _{min} \quad ^{2}_{max} \quad 0$$

results in

$$\frac{1}{2} \quad _{min} \quad _{max} \quad \sqrt{(\; _{min} + \; _{max})^2 + 4 \; ^{2}_{max}} \; :$$

□

We observe that if the system is not fully observed, then $p < (N+1)n$ and $_{min} = 0$, and the upper bound for the positive eigenvalues and the upper bound for the negative eigenvalues (23) in Theorem 6 reduces to (2.11) and (2.13) of Silvester and Wathen [35].

We are interested in how the bounds in Theorem 6 change if additional observations are introduced. The change to the upper negative bound in (22) depends on which of (23), (24) or (25) gives the bound. Hence, in Corollary 3 we comment on when (25) is larger than (24) and Corollary 4 describes a setting when the negative upper bound is given by (25).

Corollary 3.

$$\max f \; _2; \; _3 g = \; _3 \quad () \quad \frac{1}{2}(\; _{max} + \sqrt{^{2}_{max} + \; ^{2}_{min}}) \quad _{max}:$$

Proof. $\max f \; _2; \; _3 g = \; _3$ if and only if

$$\frac{1}{2} \quad _{max} \quad \sqrt{^{2}_{max} + 4 \; ^{2}_{min}} \qquad ^{1}_{max} \; ^{2}_{min}:$$

Rearranging this inequality gives

$$_{max} + 2 \; ^{1}_{max} \; ^{2}_{min} \qquad \sqrt{^{2}_{max} + 4 \; ^{2}_{min}}:$$

Squaring both sides with further rearrangement results in

$$^{2}_{min} (\; ^{1}_{max} \quad _{max} + \; ^{2}_{max} \; ^{2}_{min} \quad 1) \quad 0:$$

Since $^{2}_{min} > 0$, this is equivalent to

$$^{2}_{max} \quad _{max} \quad _{max} \quad ^{2}_{min} \quad 0;$$

from which it follows that

$$_{max} \quad \frac{1}{2} \quad _{max} + \sqrt{^{2}_{max} + 4 \; ^{2}_{min}} \; : 2, \text{this}2$$

Corollary 4. If the system is not fully observed and $\max\{\ _2;\ _3\} = \ _3$, then the upper bound for the negative eigenvalues of A_2 is given by (25).

Proof. The singular values of L and $(L^T\ H^T)$ are the square roots of the eigenvalues of $L^T L$ and $L^T L + H^T H$, respectively. Hence, by Theorem 1,

$$ {}^2_{\min} + {}_{\min}(H^T H) \quad {}^2_{\min}; $$

where ${}_{\min}(H^T H) \quad 0$, since $H^T H$ is symmetric positive semide nite. Also, if $p < (N+1)n$, then $H^T R\ ^1 H$ is singular, i.e. ${}_{\min} = 0$, and from (23) and (25)

$$ {}_1 = \frac{1}{2} \quad {}_{\max} \quad \sqrt{ {}^2_{\max} + 4\ {}^2_{\min} } \quad \frac{1}{2} \quad {}_{\max} \quad \sqrt{ {}^2_{\max} + 4\ {}^2_{\min} } \quad = \quad {}_3 = \max\{\ _2;\ _3\}: $$

□

We further describe how the negative upper bound changes if it is given by (23) or (25), including the case described in Corollary 4.

Corollary 5. If the upper bound for the negative eigenvalues of A_2 in (22) is given by ${}_1$ or ${}_3$, ${}_3$

Note that by de nition $_{\min}$ $_{\min}$ and the following inequality always holds

$$_{\min} \quad \frac{1}{2} \quad _{\min} \quad _{\max} + \sqrt{(\ _{\min} + \ _{\max})^2 + 4 \ ^2_{\min}} \ ;$$

because it can be simpli ed to

$$_{\min} + \ _{\max} \quad \sqrt{}$$

3.5 Alternative bounds

Alternative eigenvalue bounds for symmetric saddle point matrices have been formulated by Axelsson and Neytcheva [2]. These depend on the eigenvalues of the matrices $L^T D^{-1} L$, R, D and A_1, and $= \max\{|\ _i(A_1^{1/2} L^T D^{-1} L A_1^{1/2})|; i = 1, \dots, (N+1)n\}$.

Theorem 9 (From Theorem 1 (c) of Axelsson and Neytcheva [2].) The negative eigenvalues of A_3 lie in the interval

$$I_- = \left[\frac{1}{2}\left(\ _{max} - \sqrt{\ ^2_{max} + 4\ _{max}\ _{max}(A_1)}\right); \frac{1}{2}\left(\ _{min} - \sqrt{\ ^2_{min} + 4\ _{min}\ _{min}(A_1)}\right)\right]$$

and the positive ones lie in the interval

$$I_+ = \left[\ _{min}; \frac{1}{2}\left(\ _{max} + \sqrt{\ ^2_{max} + 4\ _{max}\ _{max}(A_1)}\right)\right]:$$

Note that the lower bound for the positive eigenvalues in Theorem 9 is the same as in Theorem 4.

Theorem 10 (From Theorem 1 (a) and (b) of Axelsson and Neytcheva [2].) The negative eigenvalues of A_2 lie in the interval

$$I_- = \left[-\ _{max}(A_1); -\frac{\ _{min}(A_1)}{1 + \frac{\ _{min}(A_1)}{\ _{min}}}\right];$$

and the positive ones lie in the interval

$$I_+ = \left[\ _{min}; \frac{1}{2}\left(\ _{max} + \sqrt{\ ^2_{max} + 4\ _{max}\ _{max}(L^T D^{-1} L)}\right)\right]: \qquad (34)$$

We observe that the bound (34) for the positive eigenvalues, unlike our bound in Theorem 6, is independent of the number of observations. Also, in practical applications it may not be possible to compute the upper bound for the negative eigenvalues because of the term.

4 Numerical Experiments

4.1 System setup

We present results of numerical experiments using the Lorenz 96 model [24], where the evolution of the space variables X^j; $j \in \{1, 2, \dots, n\}$, is governed by a set of n coupled ODEs:

$$\frac{dX^j}{dt} = -X^{j-2}X^{j-1} + X^{j-1}X^{j+1} - X^j + F$$

with periodic boundary conditions. In our experiments, we set $n = 40$ and $F = 8$, since the system shows chaotic behaviour with the latter value. The equations are integrated using a fourth order Runge-Kutta scheme [6]. The space increment is taken to be $\Delta x = 1/n = 2.5 \times 10^{-2}$ and the time step is set to $\Delta t = 2.5 \times 10^{-2}$. The system is run for $N = 15$ time steps.

The assimilation system is set up for identical twin experiments, i.e. the true state x^t that has Gaussian model errors $\ _i$ (described in the Section 2) is generated and observations y_i are obtained by adding noise to x^t. The error covariance matrices that are used to generate the model error in x^t and the observation error in y_i are also used for the assimilation, i.e. in the 3 3 block, 2 2 block and 1 1 block matrices. These error covariance matrices do not change over time. The observation error covariance matrix is $R_i = \ ^2_o I_{p_i}$, where p_i is the number of observations at time t_i, (diagonal R_i is a common choice in data assimilation experiments [14, 16]) and the model error covariance matrix is equal to the background error covariance matrix $Q_i = B = \ ^2_b C_b$, where C_b is a Second-Order Auto-Regressive correlation matrix [9] with correlation length scale 1.5×10^{-2}. In our experiments, the parameters are chosen so that the observations are close to the real values of the variables, and the background and the model errors are low, in particular, we set $\ _o = 10^{-1}$, which is about 5% of the mean of the values in x^t, and $\ _b = 5 \times 10^{-2}$. y_i consists of direct observations of the variables X^j; $j \in \{1, 2, \dots, n\}$ at time t_i, hence the observation operator H_i is linear.

All computations are performed using Matlab R2016b. In particular, the eigenvalues are computed using the Matlab function eig. If only extreme eigenvalues are needed, eigs is used, and the extreme singular values are given by svds

4.2 Dependence on outer loop

We first investigate whether the spectra of the matrices A_3, A_2 and A_1 depend on the outer loop of the incremental approach. In this experiment, every 4th model variable at every 2nd time step is observed. The saddle point and positive definite systems are solved using the Matlab direct solver "\". The intervals for the eigenvalues at the first 3 outer loops are presented in Table 2. Note that in these experiments, the extreme negative and positive eigenvalues oscillate around the same values throughout the outer loops and the order of change is no larger than 10^{-2}. We have run additional outer loops, but the intervals remain similar. Hence, in our subsequent experiments we consider only the first outer loop.

Matrix	1st	2nd	3rd
A_3	[2:25; 6:18 10^{2}] [1:70 10^{3}; 2:25]	[2:25; 5:97 10^{2}]	[2:25; 6:00 10^{2}]

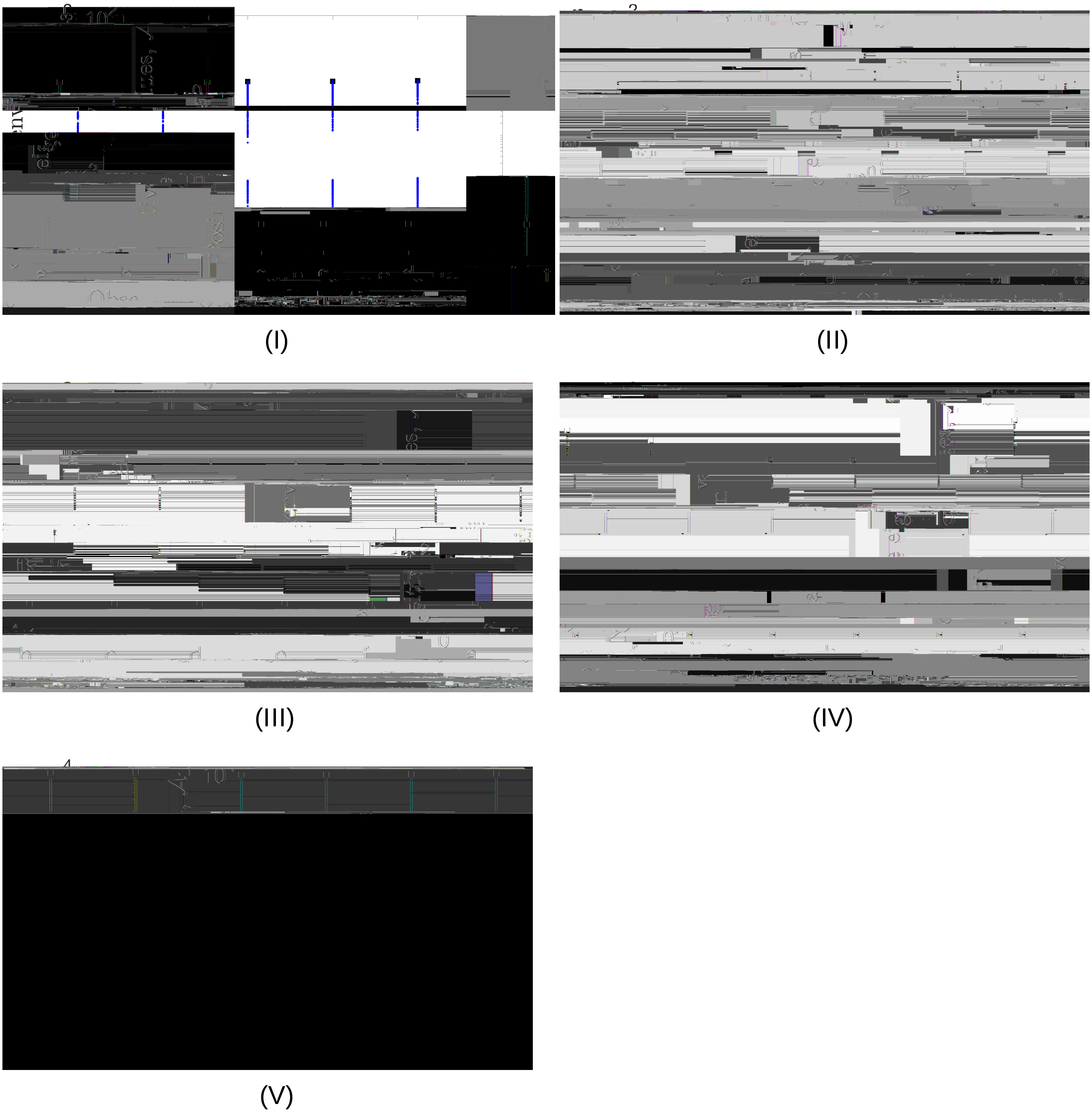

(I) (II)

(III) (IV)

(V)

Figure 1: Semi-logarithmic plots of the positive and negative eigenvalues of the matrices A_3 ((I) and (II)) and A_2 ((III) and (IV)), and the positive eigenvalues of A_1 in (V) for the different observation networks (a-f). Eigenvalues are denoted with merged blue dots. The filled black squares mark the bounds for eigenvalues of A_3 in Theorem 4, A_2 in Theorem 6, and A_1 in Theorem 8. Note that the smallest negative eigenvalues of A_2 coincide with the bounds.

Better eigenvalue clustering away from the origin when more observations are used can speed up the convergence of iterative solvers when solving the 1×1 block formulation. However, nothing definite can be said about the 3×3 block and 2×2 block formulations: the negative eigenvalues become more clustered, but the smallest positive eigenvalues approach the origin when new observations are introduced.

We also calculate the alternative eigenvalue bounds given in Theorems 9 and 10. With the choice of parameters and observations considered in this section, the bounds given in these theorems are not as sharp as those in Theorems 4 and 6. However, this is not always the case, as is illustrated in Tables 6 and 7. Here $_o = 1.5$, $_b = 1$ and the observation network d) is used.

O.n.	I	Eigenvalues	I_{+}	Eigenvalues
a)	[2:193; 2:66 10^{2}]	[2:192; 2:99 10^{2}]	[5:93 10^{4}; 2:198]	[3:56 10^{3}; 2:195]
c)	[2:249; 5:88 10^{2}]	[2:247; 6:18 10^{2}]	[5:93 10^{4}; 2:254]	[1:70 10^{3}; 2:251]
e)	[2:360; 1:28 10^{1}]	[2:358; 1:31 10^{1}]	[5:93 10^{4}; 2:365]	[1:13 10^{3}; 2:362]
f)	[2:410; 9:96 10^{1}]	[2:408; 9:96 10^{1}]	[5:93 10^{4}; 2:416]	[9:14 10^{4}; 2:413]

Table 3: Computed spectral intervals and bounds for A_3 from Theorem 4 for di erent observation networks (O.n.).

O.n.	I	Eigenvalues	I_{+}	Eigenvalues
a)	[1:0005 10^{2}; 2:83 10^{2}]	[1:0001 10^{2}; 2:99 10^{2}]	[6:03 10^{4}; 2:196]	[3:91 10^{3}; 2:195]
c)	[1:0005 10^{2}; 6:07 10^{2}]	[1:0002 10^{2}; 6:50 10^{2}]	[6:03 10^{4}; 2:196]	[1:78 10^{3}; 2:148]
e)	[1:0005 10^{2}; 1:29 10^{1}]	[1:0004 10^{2}; 1:33 10^{1}]	[6:03 10^{4}; 2:196]	[1:15 10^{3}; 2:101]
f)	[1:0005 10^{2}; 1:00 10^{2}]	[1:0005 10^{2}; 1:00 10^{2}]	[6:03 10^{4}; 5:42 10^{2}]	[9:35 10^{4}; 5:15 10^{2}]

Table 4: Computed spectral intervals and bounds for A_2 from Theorem 6 for di erent observation networks (O.n.).

O.n.	I_{+}	Eigenvalues
a)	[9:72 10^{2}; 8:11 10^{3}]	[3:23 10^{1}; 6:30 10^{3}]
c)	[4:05 10^{1}; 8:53 10^{3}]	[1:16; 6:32 10^{3}]
e)	[1:75; 9:40 10^{3}]	[5:21; 6:35 10^{3}]
f)	[1:00 10^{2}; 9:80 10^{3}]	[1:00 10^{2}; 6:40 10^{3}]

Table 5: Computed spectral intervals and bounds for A_1 from Theorem 8 with di erent observation networks (O.n.).

Eigenvalues of A_3	Bounds from Th. 4	Bounds from Th. 9
[1:93; 1:38 10^{2}]	[2:17; 5:83 10^{3}]	[5:10; 1:33 10^{2}]
[2:98 10^{1}; 3:59]	[2:37 10^{1}; 3:81]	[2:37 10^{1}; 7:53]

Table 6: Computed spectral intervals and bounds for A_3 from Theorems 4 and 9 for observation network d) with $_o = 1:5$ and $_b = 1$.

Eigenvalues of A_2	Bounds from Th. 6	Bounds from Th. 10
[1:97; 1:39 10^{2}]	[2:33; 5:83 10^{3}]	[15:79; 1:33 10^{2}]
[3:00 10^{1}; 3:51]	[2:38 10^{1}; 3:74]	[2:37 10^{1}; 7:51]

Table 7: Computed spectral intervals and bounds for A_2 from Theorems 6 and 10 for observation network d) with $_o = 1:5$ and $_b = 1$.

5 Conclusions

Weak constraint 4D-Var data assimilation requires the minimisation of a cost function in order to obtain an estimate of the state of a dynamical system. Its solution can be approximated by solving a series of linear systems. We have analysed three different formulations of these systems, namely the standard system with 1×1 block symmetric positive definite coefficient matrix A_1, a new system with a 2×2 block saddle point coefficient matrix A_2, and the version with 3×3 block saddle point coefficient matrix A_3 of Fisher and Gürol [13]. We have focused on the dependency of the coefficient matrices on the number of observations.

We have found that the spectra of A_3, A_2 and A_1 are sensitive to the number of observations and examined how they change when new observations are added. The results hold with any choice of the blocks in A_3, whereas we can only make inference about the change of the spectra of A_2

Theorem 13. Let ω_i; $i = 1; \ldots; (N+1)n + p$ be the i-th value in $\{ {}_k; {}_j | k = 1; \ldots; (N+1)n;\ j = 1; \ldots; p\}$ (the set of eigenvalues of D and R). Then the k-th eigenvalue of A_3 is bounded by

$$\text{positive eigenvalues: } \omega_k \quad {}_{max} \quad {}_k \quad \omega_k + {}_{max}; \qquad k = 1; \ldots; (N+1)n + p;$$
$$\text{negative eigenvalues: } \quad {}_{max} \quad {}_{k+(N+1)n+p} < 0; \qquad k = 1; \ldots; (N+1)n:$$

Proof. We can write A_3 as a sum of two symmetric matrices:

$$A_3 = \begin{pmatrix} D & 0 & L \\ 0 & R & H \\ L^T & H^T & 0 \end{pmatrix} = \begin{pmatrix} D & 0 & 0 \\ 0 & R & 0 \\ 0 & 0 & 0 \end{pmatrix} + \begin{pmatrix} 0 & 0 & L \\ 0 & 0 & H \\ L^T & H^T & 0 \end{pmatrix} = S_D^{3x3} + S_L^{3x3}:$$

The spectrum of S_D^{3x3} is the union of the eigenvalues of D, R and zeros. By Theorem 12, the eigenvalues of the inde nite matrix S_L^{3x3} are the singular values of $(L^T\ H^T)$ with plus and minus signs, thus ${}_{min} = \quad {}_{max}$ and ${}_{max} = \quad {}_{max}$.

The result follows from applying Theorem 1 to the matrices S_D^{3x3} and S_L^{3x3}. □

Theorem 14. The eigenvalues of A_2 are bounded by

$$\text{positive eigenvalues: } {}_k \quad {}_{max} \quad {}_k \quad {}_k + {}_{max}; \qquad k = 1; \ldots; (N+1)n:$$
$$\text{negative eigenvalues: } {}_k \quad {}_{max} \quad {}_{k+(N+1)n} \quad {}_k + {}_{max}; \qquad k = 1; \ldots; (N+1)n; \tag{35}$$

Proof. As in Theorem 13, we express A_2 as a sum of two symmetric matrices

$$A_2 = \begin{pmatrix} D & 0 \\ 0 & H^T R\ ^{1} H \end{pmatrix} + \begin{pmatrix} 0 & L \\ L^T & 0 \end{pmatrix} = S_D^{2x2} + S_L^{2x2}:$$

The rest of the proof is analogous to that of Theorem 13. □

Corollary 9. If there are $p < (N+1)n$ observations, (35) in Theorem 14 becomes

$${}_{max} \quad {}_{k+(N+1)n} \quad 0; \qquad k = 1; \ldots; (N+1)n \quad p;$$
$${}_k \quad {}_{max} \quad {}_{k+2(N+1)n \quad p} < \quad {}_k + {}_{max}; \qquad k = 1; \ldots; p:$$

Proof. The result follows from noticing that $H^T R\ ^{1} H$ has $(N+1)n \quad p$ zero eigenvalues. □

References

[1] Andersson, E., and Th epaut, J.-N. Assimilation of operational data. In Data Assimilation. Making Sense of Observations

[10] El-Said, A. Conditioning of the weak-constraint variational data assimilation problem for numerical weather prediction. PhD thesis, Department of Mathematics and Statistics, University of Reading, 2015. PhD thesis.

[11] Elbern, H., Schmidt, H., and Ebel, A. Variational data assimilation for tropospheric chemistry modeling. Journal of Geophysical Research: Atmospheres 102, D13 (1997), 15967 { 15985.

[12] Fisher, M. Minimization algorithms for variational data assimilation. In Proceedings of the Seminar on Recent Developments in Numerical Methods for Atmospheric Modelling (1998), European Centre for Medium Range Weather Forecasts, pp. 364 { 385.

[13] Fisher, M., and Gürol, S. Parallelisation in the time dimension of fimi8dimensi and Ebel, A.

[33] Saad, Y. Iterative Methods for Sparse Linear Systems, 2nd ed. Society for Industrial and Applied Mathematics, 2003.

[34] Saad, Y., and Schultz, M. H. GMRES: A generalized minimal residual algorithm for solving nonsymmetric linear systems. SIAM Journal on Scientific and Statistical Computing 7, 3 (1986), 856 { 869.

[35] Silvester, D., and Wathen, A. Fast iterative solution of stabilised Stokes systems. Part II: using general block preconditioners. SIAM Journal on Numerical Analysis 31, 5 (1994), 1352 { 1367.

[36] Silvester, J. Determinants of block matrices. Mathematical Gazette 84, 501 (2000), 460 { 467.

[37] Simoncini, V., and Szyld, D. B. On the superlinear sonvergence of MINRES. In Numerical Mathematics and Advanced Applications 2011. Proceedings of ENUMATH 2011 (2013), A. Cangiani, R. Davidchack, E. Georgoulis, A. Gorban, J. Levesley, and M. Tretyakov, Eds., Springer, pp. 733 { 740.

[38] Stewart, G., and Sun, J.-G. Matrix Perturbation Theory. Computer Science and Scientific Computing. Academic Press, 1990.

[39] Swinbank, R. Numerical weather prediction. In Data Assimilation. Making Sense of Observations, W. Lahoz, B. Khattatov, and R. Menard, Eds. Springer-Verlag Berlin Heidelberg, 2010, pp. 381 { 406.

[40] Talagrand, O. Variational assimilation. In Data Assimilation. Making Sense of Observations, W. Lahoz, B. Khattatov, and R. Menard, Eds. Springer-Verlag Berlin Heidelberg, 2010, pp. 41 { 68.

[41] Trefethen, L. N., and Bau, III, D. Numerical Linear Algebra. SIAM, 1997.

[42] Tr emolet, Y. Accounting for an imperfect model in 4D-Var. Quarterly Journal of the Royal Meteorological Society 132, 621 (2006), 2483 { 2504.

[43] Tr emolet, Y. Model-error estimation in 4D-Var. Quarterly Journal of the Royal Meteorological Society 133, 626 (2007), 1267 { 1280.